2022

Energy as a Limiting Factor in Neuronal Seizure Control: A Mathematical Model

Sophia E. Epstein
Claremont McKenna College

Energy as a Limiting Factor in Neuronal Seizure Control:

A Mathematical Model

A Thesis Presented

by

Sophia Epstein

To the Keck Science Department

of

Claremont McKenna, Scripps, and Pitzer Colleges

In Partial Fulfillment of

The Degree of Bachelor of Arts

Senior Thesis in Neuroscience

25 April 2022

Acknowledgements

I would like to extend my deepest gratitude to my advisor, Professor John Milton. Thank you for cultivating my curiosity in dynamical neuroscience and its applications. I am unbelievably appreciative for the countless Zoom brainstorming discussions and the stream of recommended articles. Additionally, I would also like to thank Professor Michael Spezio for his useful critiques and encouragement. Professor Sam Nelson, thank you for helping ground my theoretical neuroscience in strong computational mathematics.

To my friends and family, thank you for always entertaining and supporting my passions. You all played an integral role in this process, from proofreaders to soundboards to moral support and encouragement to step away from my computer. Specifically to my parents, thank you for providing me with unwavering love and support.

Abstract

The majority of seizures are self-limiting. Within a few minutes, the observed neuronal synchrony and deviant dynamics of a tonic-clonic or generalized seizure often terminate. However, a small epilesia partialis continua can occur for years. The mechanisms that regulate subcortical activity of neuronal firing and seizure control are poorly understood. Published studies, however, through PET scans, ketogenic treatments, and in vivo mouse experiments, observe hypermetabolism followed by metabolic suppression. These observations indicate that energy can play a key role in mediating seizure dynamics. In this research, I seek to explore this hypothesis and propose a mathematical framework to model how energy may limit seizure propagation. Expanding upon existing models of neuronal spiking and energy consumption, the model accounts for change in available energy over time. The results of this model indicate constrained energy consumption is a plausible mechanism for mediating seizure termination.

Contents

Chapter 1

Introduction

Over 50 million people worldwide suffer from epilepsy [63]. Given its prevalence in society, significant research has begun into epilepsy and seizures. In the past ten years alone there has been the introduction of new treatment options, ways of measuring seizure behavior, understanding of comorbidities, and insight on seizure emergence [77]. Despite significant progress and a flood of new pharmaceuticals in the market, one third of patients have drug resistant medically refractory epilepsy [34]. For these patients, there has been promising research on the effects of the ketogenic diet and brain stimulation. Yet, it is unknown why the ketogenic diet works.

In working to treat seizures, it is critical to note that the majority of seizures are self limiting, lasting only a few minutes. If one can gain an understanding of how seizures self regulate, treatment options can be modeled from biological mechanisms. However, the mathematical modeling of seizure termination is under studied [33]. Thus far, studies on the mechanisms of seizure termination take two main approaches. The first approach focuses on metabolic mechanisms such as ionic concentration, acidity, or neuromodulator

release and dependence on neuronal activity [82]. The second approach employs functional networks from electrophysiological recordings to analyze these methods without detailed accounts of cellular biology. Little work has been done to synthesize these two approaches to further understand seizure termination.

This thesis incorporates metabolic mechanisms into a model of neural activity in order to investigate how seizures terminate. Chapter 2 provides background information on epilepsy, energy in neuronal function, and energy metabolism during seizures. Additionally, it cites existing mathematical models of epilepsy and neuronal computational expenditures. Chapter 3 introduces the model (equations and parameters) and its assumptions. Using this model, Chapter 4 explains its implications and dynamical behavior. Then, the paper discusses how this model can be further expanded/modified to increase accuracy, as well as its commentary on existing phenomena and treatment methods in Chapter 5.

Chapter 2

Background

2.1 Epilepsy as a Disorder

Epilepsy is a symptom of neurological dysfunction. It comes in many forms with a vast array of underlying causes. In literature, epilepsy is broadly classified as a central nervous system disorder which places someone at a predisposition to generate/develop an epileptic seizure. More generally, it causes paroxysmal alteration of brain activity due to the hyper-synchronous discharge of neurons in the brain [52]. This leads to abnormal periods of activity. The International League Against Epilepsy distinctively defines epilepsy as any of the following: 1) two or more unprovoked seizures occurring $24hr$ apart; 2) one unprovoked seizure with a probability of future seizures (a high recurrence risk) in the next 10 years after two prior seizures occurring; or 3) a diagnosis of epilepsy syndrome [46].

2.1.1 Prevalence

Epilepsy is one of the most common disabling neurological conditions, with 50 to 120 new cases per year per 100,000 people [16]. Approximately three million people in the US and 50 million people world wide are affected by this disease [23]. Acute symptomatic seizures are predominately seen in patients under one year of age and in the elderly. Within age groups under one year of age there was 86 per 100,000 well documented cases per year, 23-31 per year in people ranging in age from 30-59, and 180 per 100,000 cases per year in individuals over 85 [66] [7]. Incidence of epilepsy appears to be higher in low/middle-income countries and communities due to perceived greater exposure to risk/ethological factors as well as methodological issues [62]. Additionally, prevalence appears to be slightly higher in men than women. While this distinction is poorly understood, it is believed that differences may be explained by prevalence of common risk factors and the socio-cultural reasoning in women to conceal such conditions.

2.1.2 Mortality

Standardized mortality rates are seen to be two to three times higher in those with epilepsy compared to others [59]. This excess mortality is often attributed to the underlying cause of epilepsy and not epilepsy itself. Some excess deaths can be attributed to seizures, the accompanied increased risk of accidents, sudden unexpected/unexplained deaths (SUDEP), and suicide [22]. Sudden unexpected death in epilepsy rates are correlated to the severity of epilepsy with only 1 per 2500 in mild epilepsy to 1 per 100 in severe and intractable epilepsy [25]. Death rates are significantly higher in the first few years after diagnosis. Studies have suggested that life expectancy estimates are reduced by two years in those with

idiopathic/cryptogenic epilepsy and up to 10 years in those with symptomatic epilepsy.

2.1.3 Comorbidities

Comorbid conditions are highly common for individuals with epilepsy. Mood disorders are the most common comorbidities, but other psychiatric and physical conditions are also frequently present [49]. This includes significantly increased rates of depression, anxiety, attention deficit hyperactivity disorder, autism spectrum disorder, developmental delays, Alzheimer's disease, and conduct disorders [6]. Neurological comorbidities include migraines, premature mortality, and cognitive impairments [65]. Physical disorders include musculoskeletal system disorders, gastrointestinal disorders, respiratory disorders, chronic pains, obesity, diabetes, infections, and allergies.

2.1.4 Causes

The causes of epilepsy are still not fully known, however they can be divided into four main categories [67]:

1. Idiopathic Epilepsy: Idiopathic epilepsy is due to a predominately genetic origin in which there is no prevalent underlying abnormality identified.
2. Symptomatic Epilepsy: Symptomatic epilepsy is likely due to an acquired or genetic cause attributed with neuro-anatomical or neuro-pathological abnormalities which indicates a disease or condition.
3. Provoked Epilepsy: Provoked epilepsy is due to a specific identifiable systemic or environmental factor which causes seizures.
4. Cryptogenic Epilepsy: Cryptogenic epilepsy emerges due to an unknown cause which

has not been identified.

2.1.5 Treatment Options

Epilepsy is predominately a treatable condition. Up to 80% of individuals enter periods of seizure remission [21] [6]. However, less than 50% of cases achieve prolonged periods of seizure remission. These remission patterns are poorly understood. There are three primary modes of treatment [41].

Altering Electrical Activity

Electrical activity can be altered on the microscale of ionic channels or on a network scale.

Antiepileptic medication can affect ion channels in the cell membrane. Ion channels play a critical role in neuronal function [10]. Voltage gated sodium channels are responsible for initiation and propagation of excitatory signals. Voltage gated calcium channels similarly mediate a neurons response to depolarization (release of neurotransmitters and regulation of neuronal excitability). Voltage gated calcium channels mediate excitability of a cell via establishing resting membrane potential. Voltage-gated chloride channels regulate excitability and acidification of synaptic vesicles.

On a network scale, energy can be altered through deep brain stimulation or transcranial magnetic stimulation [71]. Primary regions targeted include the vagus nerve, thalamus nuclei, hippocampus, subthalamic nucleus, and cerebellum. While the exact mechanisms of action is unknown, the energy requirement for neurons to respond to a stimulation may provide a plausible theory.

Altering Chemical Transmission

To alter chemical transmission between neurons, anti-epileptic drugs frequently target neurotransmitters in synapses and their corresponding receptors. Neurotransmitter supply and demand has played a key role in epileptic seizure dynamics.

Generally, it is believed that excitatory glutamatergic neuro-transmission may be partially responsible for the initiation and spread of seizure activity. In a similar manner γ-aminobutyric acid (GABA) synaptic inhibition is critical in regulating seizure activity by preventing hyperactivity [8]. Thus, any dysfunction in GABA or glutimate availability would have consequences on seizure genesis. Common pharmacological treatments for epilepsy result in the blockade of glutamine production or uptake [68]. This is due to the pathway where gultamine is a precursor glutimate which is a precursor for GABA synthesis. Many antiepileptic drugs function via altering GABA availability [51]. A few common drugs include benzodiazepine, barbiturates, and GABA transminase [60]. Benzodiazepine receptor agonists function as a positive allosteric modulator. Functionally, they enhance action of GABA via altering the frequency of channel openings which increases GABA sensitivity. Given the mode of function benzodiazepines lead to a myriad of side effects and have diminishing effectiveness over time. Barbiturates also act of allosteric modulators of GABA receptors by shifting the relative proportion of GABA-induced channel openings to favor the longest lived open state. GABA transaminase directly enhances inhibitory neurotransmitter via aiding the breakdown of GABA.

Removal of Seizure Focus

Surgery is a last resort option for patients who have severe drug resistant seizures. Despite its potential for complications, it is seen to most effectively prevent seizures. For those

with focal epilepsy, if the epileptogenic zone can be located, surgical resection may be a treatment option. A less invasive surgery may be laser interstitial thermal therapy which uses a laser to destroy a portion of brain tissue. Corpus callosotomy, hemispherectomy, and functional hemispherectomy are among more drastic measures of disconnecting larger regions of the brain for seizure control.

2.1.6 Seizure Types

The classification of epilepsy seizures encompasses a vast array of neuronal activity. There are three main categories of seizures: generalized, focal, and epileptic spasms. Generalized seizures effect the brain bilaterally. Focal seizures originate in small neural networks and are isolated to one region of a cerebral hemisphere.

Originally epileptic seizures were defined and classified based on the associated behavioral event. These behavioral events include flushing, muscle twitching, convulsions, or shifts in attention. Based on these differentiating metrics, seizures were classified into tonic-clonic, absence, atonic, myoclonus, or epileptic spasms. Tonic-clonic seizures typically begin on both sides of the brain with muscle stiffening and altering levels of consciousness (known as the tonic phase). Once the tonic phase is complete, the clonic phase causes rapid jerking of the limbs. Absence seizures are characterized solely by a lapse in consciousness. In an atonic seizure muscles become weak/limp. Myoclonus seizures are categorized by brief periods of muscle twitching. Epilleptic spasms are when the body flexes and extends repeatedly and rapidly. However, this method of defining seizures led to significant uncertainty due to the overlap in classification criteria and difficulties in deciphering presenting symptoms. Instead today these labels are believed to be symptoms of a seizure. The development of the Electroencephalogram (EEG), a method of mea-

suring brain electrical activity, led to the adoption of the definition of seizures as a temporary dysfunction of the brain due to excessive synchronous neuronal discharge (firing). Thus, seizures exist on this continuum of spatial (number of channels) and rate (amplitude and frequency) dependencies from a large seizure, small seizure, minimal seizure, and no seizure. The dynamics of a seizure, however, vary significantly. This led to the development of many subsequent sub classes: generalized onset seizure (effects both sides of the brain at the same time), focal onset (starts in one area/group of cells in the brain), and unknown onset (when the origin of the seizure is unknown).

2.1.7 Dynamical Characteristics of Epilepsy

One can define the brain as a multi-dimensional dynamical system with a random independent set of system variables and parameters evolving in time and across different time scales. In this context, it becomes clear how epilepsy can be described as a dynamical disease which evolves over time [40]. A dynamical disease is one in which exhibits changes in qualitative dynamics as a parameter changes, causing a bifurcation [19]. Specific to the nervous system, it is a disease that emerges from an abnormality in some existing neural control mechanism [4]. Epileptic seizures are ”transient clinical manifestations that result from an episode of epileptic neuronal activity” [72]. Epileptic neural activity references a specific dysfunction of abnormal synchronization, excessive excitation or insufficient inhibition, and can aggregate across varying spatial scales. Approaching epileptic seizures on a broad scale of latent periods followed by seizing states, brain state transitions from one attractor state to another within the multi-stable dynamical landscape occur due to some perturbation in at least one parameter. Current mathematical focus of seizure onset and offset focuses on a codimension one system where one parameter is sufficient to cause a

bifurcation although it is possible for naturally occurring seizures to reflect changes in two or more parameters [61] [28].

Through experimental studies, the basic building blocks to seizure like events (SLEs) which establish these multi-stable dynamical landscapes have been established. Neurons and neural populations are examples of "fast-slow" dynamical systems, as they involve two types of dynamical variables evolving on very different time scales (see Figure 2.1) [45] [27].

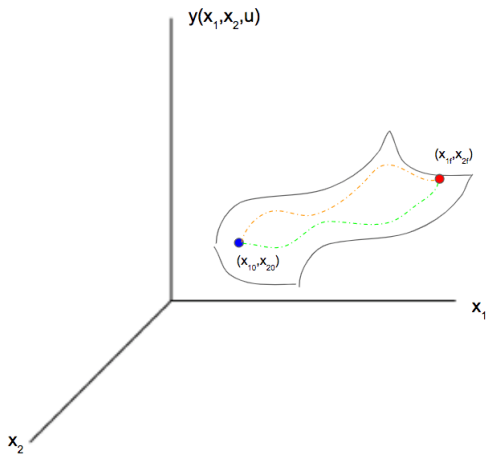

Figure 2.1: A sample geometric interpretation of a fast-slow dynamical system problem. $y(x_1, x_2, u)$ represents the cost exhibited at various state and input combinations. x_2 represents the fast dynamics, while x_2 represents the slow ones. Considering this as an optimization problem, (x_{10}, x_{20}) represents the initial state of the system and (x_{11}, y_{21}) represents the desired state [26].

Mathematically a fast-slow ordinary differential equation (ODE) can be written in the form

$$\xi \dot{x} = f(x,y),$$

$$\dot{y} = g(x,y),$$

such that the components of $x \in \mathbb{R}^n$ are fast variables $y \in \mathbb{R}^m$ are slow variables, and ξ is a

parameter.

Typically the two time scales that arise during SLEs are due two interacting processes involving fast-slow currents. On the most basic level of a single neuron, SLEs can be characterized by a beginning onset, numerous sequences of rapid discharges and spike wave events (SWEs), and the ending offset. At onset, a SLE's abrupt appearance of fast discharges scaling up from a non-zero value indicates either a subcritical Hopf bifurcation or a saddle node bifurcation with a baseline shift on the time-dependent voltage [30]. The disappearance or emergence of a fixed point due to changes in parameter values is known as a bifurcation. A fixed point is the point at which all differential equations are equal to zero and therefore intersect. In a subcritical Hopf bifurcation there exists an unstable cycle surrounding a stable equilibrium point. In comparison a saddle node bifurcation has a collision and disappearance of two equilibria in dynamical systems. These two theories for dynamical behavior of SLE onset explain different aspects of seizure initiation [70].

During the ictal period of seizure behavior, the dynamics vary significantly and are impossible to accurately model with a single bifurcation diagram. Once then approaching offset, many seizures are self terminating lasting only a few minutes in length. The termination dynamics illustrate a direct current shift back towards baseline resting state. This indicates a saddle homoclinic bifurcation due to the maintenance of a non-constant frequency towards seizure offsets [30]. Homoclinic bifurcations includes a homoclinic orbit whose trajectory approaches a fixed point both as $t \to \infty$ and $t \to -\infty$ which forms as the parameter is varied. This means, as the parameter is varied a periodic orbit is either created or destroyed.

2.2 Role of Energy in Neuronal Function

While it has been difficult to observe the exact mechanisms of human brain energy consumption, it has been determined it increases proportionally to the number of neurons across different species. This allows for conclusions to be made from deriving data from in vivo experiments and studies [11]. In normal states metabolic consumption of the brain represents over 20% of the whole body oxygen uptake [37]. During these conditions, the primary energy substrate in the brain is blood derived glucose. Via the glycolytic pathway two pyruvates and two ATP molecules are generated from one molecule of glucose. This pyruvate can then either be reduced to lactate or enter the Krebs cycle which will generate approximately 29 additional ATP molecules per single glucose. These ATP sources will change dynamically in response to neuronal activity. To some extent, neuronal mitochondria can raise ATP synthesis in response to increased synaptic stimuli (within max production abilities and sufficient resources). The Na+ pump may also rapidly increase ATP synthesis of the mitochondria. As seen via PET scans, neuronal activity may elicit local increase in blood flow, glucose uptake, and oxygen.

ATP production for neurons is critical during signaling. It has been estimated that 75% of gray-matter energy is used in signaling to restore ion gradients [2]. Other energy expenditures comes from the demanding process of propagating action potentials along an axon and general synaptic activity [75].

A simple mathematical model for ATP metabolism in the brain can be proposed [76] :

$$\frac{\mathrm{d}G_{ATP}}{\mathrm{d}t} = S(t, G_{ATP}, \ldots) - C(t, G_{ATP}, \ldots)\,, \tag{2.1}$$

where $S(t, G_{ATP}, \ldots)$ is a function representing the sum of all rate of reactions that syn-

thesize ATP. Conversely, $C(t, G_{ATP}, \ldots)$ is a function of the sum of all reaction rates that consume ATP. Note, these functions will depend on both time and the level of available ATP. At a homeostasis, $0 = S(t, G_{ATP}, \ldots) - C(t, G_{ATP}, \ldots)$ indicating $S(t, G_{ATP}, \ldots) = C(t, G_{ATP}, \ldots)$. However, how dynamic can ATP production be?

Scientists have been concerned with energy factors in seizures for quite a significant time. Initially, as summarized in 1965, research focused on determining if energy metabolism in a given epileptic focus varied from the rest of the brain [32]. Hughling Jackson, in 1867, described epilepsy as a "sudden disorderly expenditure of force and energy" comparing it to regional palsy and spasms [29]. Recently, the limits of ATP plasticity have been observed in numerous proxy species studies. In these experiments heightened firing rates, in a seizure state or during a learning task, were presumed to require increased energy [37]. Most notably, in Mery and Kawecki's article [39] experimental fruit flies were conditioned to develop long term memories, meaning increased cortical computation and firing rates. Upon starvation, these flies died 20 % quicker than the control flies presumably due to the costs associated with increased cortical computation. A corollary study also revealed during these periods of increased neuronal activity, fruit flies independently consumed double the amount of sucrose [58]. While brain energy consumption does increase with brain size, brain energy consumption increases proportionally to the number of neurons among different species, including humans [76].

2.3 Energy Metabolism during Seizures

2.3.1 ATP Availability

During a seizure the metabolic rate of glucose and oxygen significantly increase [78]. However, it is believed that the main aerobic pathway, the TCA cycle, does not supply enough energy. Thus, glycolysis becomes a main supplier of neuronal ATP [79]. This hypothesis emerged to explain the decreased levels of TCA cycle related enzymes (aconitase, malate dehydrogenases, and succinate dehydrogenases) and the increase in anaerobic glycolytic metabolic enzymes (phosphofructokinase and glucose kinase) [18] [1]. This increased activity also is associated with an increase in lactic acid production. In theory, in this hypoxic state, lactate can be harvested from sources, converted into pyruvate , and directed back into glycolysis [42] [5]. This increase in anaerobic glycolysis could help contribute the energy supply to sustain exaggerated seizure firing.

2.3.2 Changes in Cerebral Blood Flow: Metabolic Analysis via Positron Emission Tomography Scans

Positron emission tomography(PET) scans are a sensitive nuclear medicine method of imaging energy metabolism in the brain. The metabolism of the selected radio-pharmaceutical is measured via the detection of photons emitted by a radionuclide in the organ/tissue of interest. Radionuclide is administered through an IV line. Positrons are emitted via the breakdown of radionuclide. When these positrons collide, they release gamma rays known as annihilation photons. These annihilation photons are measured by a scanner. Given the nature of their measurements, PET imaging has been particularly useful in measuring

seizure disorders.

Neurons derive their energy exclusively from the uptake of glucose. $[^{18}F]$ Fluoro-2-deoxyglucose can be taken up by neurons, but cannot be metabolized by them. In this way, PET provides a measurement that is proportional to metabolic requirements of the neuron.

As described earlier, during an epileptic seizure cerebral metabolism and blood flow are significantly increased in engaged brain regions. This has been observed in PET scan analysis of seizures. For generalized seizures, cross cortical hypometabolism and interictal minor depression is indirectly observed using radio-pharmaceutical fluorine-18-fluorodeoxyglucose. For focal partial seizures, FDG-PET enabled the identification of seizure foci and subsequent relative depression states. While research has focused on this hypermetabolism in localized brain regions as a means of detecting seizure foci, little attention has been directed towards correlated regions of hypometabolism. During the ictal period of a seizure, a region of hypometabolism accompanies the hyper-metabolism (see Appendix A) [14]. Hypometabolism in seizures never is presented in isolation. From an energy consumption perspective, this could indicate a reallocation of energy metabolism from one region to propagate and maintain a seizure. Supporting this hypothesis, in localized seizures upon immediate entering the the post-ictal stage studies observed a hypometabolic area confined to the epileptogenic zone. Yet, in widespread limbic seizures with convulsions, the epileptogenic zone was not the only region of hypometabolism. Other regions with decreased activity included the cerebellum (which is the primary consumer of the brains energy). Patients with tonic posturing, or sustained flexation of the muscles, exhibited widespread cerebellar and parietal lobe reductions [64]. This observed decrease can explain both a energy depletion causing the seizure to end and a reallocation from other regions which enabled the seizure to be sustained for that period.

2.3.3 Energy During Post-Ictal States

Ketogenic Diet and Seizure termination

Since the 1920s the ketogenic diet has been successfully used to primarily treat young children with intractable epilepsy. Under the ketogenic model patients consume high fat, low carbohydrates, and adequate protein. Despite its apparent success, it is not palatable or sustainable. The hope is that the mechanism of the ketogenic diet can be accomplished in an alternative way without so many severe side effects and limitations. The composition of the four major types of ketogenic diets are illustrated in Table 2.1.

Table 2.1: Common ketogenic diet macronutrient compositions

Ketogenic Diet	Fat (g)	Protein (g)	Carbohydrate (g)	Fat calories (% of total)
Classic	100	17	8	90
MCTD	78	25	50	70
MAD	70	60	10	70
LGIT	60	40	40	45

Traditionally carbohydrates are the primary sources of energy production in the body. However, when the body is denied carbohydrates it enters a catabolic state of gluconeogenesis and ketogenesis due to decreased insulin secretion.

Gluconeogenesis generates glucose from non-carbohydrate carbon substraights. Each molecule of glucose is synthesized from two pyruvate molecules, four ATP, two GTP, and two NADH [12]. This is significantly less efficient that standard glucose breakdown.

As glucose availability drops further, the endogenous production of glucose can not keep up with the body's need for energy sources. In order to provide alternative sources of energy the body undergoes ketogenesis to replace glucose with ketone bodies as a primary source of energy. Ketogenesis produdces acetone, acetoacetate, and β - hydroxybutyrate

molecules via the breakdown of fatty acids [12]. The reaction of the ketone bodies are as follows:

$$2\text{Acetyl CoA} \rightarrow \text{Acetoacetyl CoA} + \text{coASH},$$

$$\text{Acetyl CoA} + \text{Acetoacetyl CoA} \rightarrow \beta - \text{Hydroxy-}\beta\text{-methyglutaryl CoA},$$

$$\beta\text{-Hydroxy-}\beta\text{-methyglutaryl CoA}, \rightarrow \text{Acetoacetate} + \text{acetyl CoA},$$

$$\text{Acetoacetate} + \text{NADH} \leftrightarrow \beta\text{-Hydroxybutyrate} + \text{NAD},$$

$$\text{Acetoacetate} \rightarrow \text{Acetone} + \text{CO}_2.$$

For as long as the body is deprived of carbohydrates, the metabolism remains in a ketogenic state. Unlike fatty acids, which cannot pass the blood brain barrier, enzymes in the brain make it possible for ketone enzymes to be extracted and used. In the brain ketone bodies can be concerted into acetyl-CoA which enter the TCA cycle leading to the eventual production of ATP. The reactions of ketone body degradation are:

$$\beta\text{-Hydroxybutyrate} + \text{NAD} \leftrightarrow \text{Acetoacetate} + \text{NADH} + \text{H}^+,$$

$$\text{Acetoacetate} + \text{succinyl CoA} \leftrightarrow \text{Acetoacetyl CoA} + \text{succinate},$$

$$\text{Acetoacetyl CoA} + \text{CoASH} \leftrightarrow 2\text{Acetyl CoA}.$$

The exact anti-seizure mechanisms of the ketogenic diet are unknown, however it is believed polyunsaturated fatty acids and ketone bodies play a critical role.

If the energy metabolism and synaptic function hypothesis is true, energy availability plays a clear role sustaining in seizure activity [20]. On a ketogenic diet, the blood glucose

energy levels are extraordinarily low. The brain then uses ketone bodies for energy. Since aerobic exercise is an inefficient process, the body has reduced energy availability. In return, this blocks seizure activity. As observed in in vivo experimental trials, anti-convulsant effects of the ketogenic diet were immediately reversed via a glucose infusion [69]. The sudden availability of glucose as an energy source, enables the preservation and initiation of seizure activity.

Antiepileptics

Recently due to the widespread success of the ketogenic diet, there has been increasing research on drugs that affect metabolic pathways as treatment options [15]. To directly mimic the ketogenic diet, a glycolysis inhibitor 2-DG can be exployed. Its mechanism of reducing epileptic seizures may be due to the activation of a K_{ATP} channel which decreases intracellular ATP concentration (subsequently increasing extracellular ATP concentration). Another potential mechanism may be due to its reduction of the brain-derived neurotropic factor and its receptor TrkB which reduces neuron hyper-excitability. Lastly, it effects the concentration of nicotinamide adenine dinucleotide phosphate which results in the potentiating GABAergic tonic inhibition [56].

2.4 Related Literature

2.4.1 Epilepsy Models

Computational models of epilepsy exist in literature in many forms [70]. Here I model an epileptic neuron using models that generate a burst of spiking activity of varying duration. There are only four possible codimension one bifurcations for the onset of a burster and

only four possible codimension one bifurcation for the offset of a burster [27]. In other words, there are only 16 possible variations in total. One of these possibilities is exhibited by the Chay model for a neuronal burster considered in Section 2.4.2.

From these bursters, some existing models have suggested preliminary estimates of computational costs in neuronal spiking.

2.4.2 Energy Models

The Cost of Cortical Computation

Lennie in "The Cost of Cortical Computation" investigates the cost of an individual spike of a cortical neuron. He provides a rough estimate for this value [35] . Lennie's model is based on an earlier model proposed by Attwell and Laughlin of energy requirements for a spiking neuron in mice [2]. Using the same calculations and formulas, Lennie adopts parameters to explain human dynamics. His model breaks down the energy calculations into individual biological components to a neural spike: an action potential, post synaptic glutamate, refractory period, and glutamate recycling.

Chay Model

The Chay Model has been used to simulate bursting activities of neurons, focusing on ionic currents of sodium-calcium mixed channel ions, voltage depending potassium currents, calcium dependent potassium channel ions and leakage [9]. The Chay model was selected to represent neuronal dynamics due to its bursting nature. The most common mathematical model of epilepsy is the Epileptor. It suggests a simplifying assumption of characterizing a seizure as an arbitrary long bursting pattern with the two states being refractory status

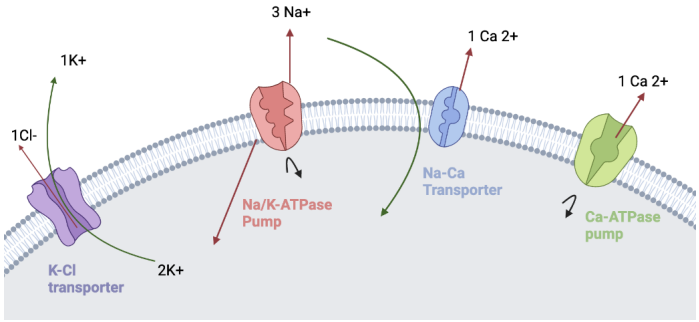

Figure 2.2: Diagram of the major ion pumps and transporters in the Chay model. Red arrows are representative of ion movement against the gradient and green is along the gradient. Black arrows represent the hydrolysis of ATP.

epilepticus (RSE) and depolarization block (DB) [13]. Mathematically it can be represented with three differential equations:

$$\frac{dV}{dt} = g_i m_\infty^3 h_\infty (V_i - V) + g_{kv} n^4 (V_k - V) + g_{kc} \frac{C}{1+C} (V_k - V) + g_l (V_l - V) + I, \tag{2.2}$$

$$\frac{dn}{dt} = \frac{n_\infty - n}{\tau_n}, \tag{2.3}$$

$$\frac{dC}{dt} = \rho (m_\infty^3 h_\infty (V_C - V) - k_C C), \tag{2.4}$$

where for $y \in [m,h,n]$, $y_\infty = \frac{\alpha_y(V)}{\alpha_y(V)+\beta_y(V)}$. For $y = m$, $\alpha_m(V) = 0.1(25+V)/(1-e^{-0.1V-2.5})$, and $\beta_m(V) = 4e^{-(V+50)/18}$. For $y = h$, $\alpha_h(V) = 0.07e^{-0.05V-2.5}$, and $\beta_h(V) = 1/(1+e^{-0.1V-2})$. For $y = n$, $\alpha_n(V) = 0.01(20+V)/(1-e^{-.1V-2})$ and $\beta_n(V) = 0.125e^{-(V+30)/80}$. Also, $\tau_n = 1/(\lambda_n(\alpha_n + \beta_n))$. Where V = membrane potential, n = probability of a voltage dependent K^+ channels, and C is the intracellular Ca^{2+} concentration. V_i, V_k, V_c, and V_l are reversal potentials for mixed $Na^+ - Ca^{2+}$, K^+, Ca^{2+} and leakage ions. g_i, g_k, g_c, and g_l represent the maximum conductance of the same ions respectively. m_∞ and h_∞ are probabilities of activation and inactivation of the mixed inward current channel. n_∞ is the

steady-state value of n, τ_n is the relaxation time of the voltage-gated K^+ channel. k_C is the rate constant corresponding to the efflux of intracellular Ca^{2+}, and ρ is the respective proportionality constant. I is the stimulus current.

Using the framework of Chay model, Zhu Wang et al propose energy consumption calculations.

$$P = |I_{kv}V_k| + |I_{kc}V_K| + |I_lV_l| - |I_iV_i|, \tag{2.5}$$

such that:

$$\begin{aligned} I_i &= g_i m_\infty^3 h_\infty (V - V_i), \\ I_{kv} &= g_{kv} n^4 (V - V_k), \\ I_{kc} &= g_{kc} \tfrac{C}{1+C} (V - V_k), \\ I_l &= g_l (V - V_l). \end{aligned}$$

Zhu Wang et al indicate that during spontaneous firing energy consumption arises from active ionic transport. ATP consumed by ionic pumps is transformed into the energy in the form of transmembrane concentration gradients of each ions, also known as reversal potential [80]. Thinking of the electrical properties of a neuron as a circuit, reversal potentials a voltage, and as a result, I_x for $x \in \{i,k,l\}$ as current (B.1).

In this framework, the energy calculated is solely due to the Na/K-ATPase pump. ATP consumed by the CP-ATPase pump was ignored because it is insignificant, from the energy consumption perspective, in the context of the Chay Model (a mixed $Na^+ - Ca^{2+}$) with very low changes in concentration. To obtain the total amount of energy consumed by a bursting neuron during time t, one can calculate $\int_0^t P dt$.

Chapter 3

Materials and Methods

3.1 New Models

Existing models have been created to explore single neuron energy consumption in gray matter of mice. However, little work has been made to adapt these models and their parameters to explain human seizure dynamics [2]. The model presented below will derive a model to explain the dynamics of cortical computation and ATP availability.

3.1.1 Single Neuron Model

As a simple model, the rate of energy can be calculated by the rate of ATP production minus the rate of ATP consumption,

$$\frac{\mathrm{d}G_{ATP}}{\mathrm{d}t} = S(t, G_{ATP}, \ldots) - C(t, G_{ATP}, \ldots). \tag{3.1}$$

where $S(t, G_{ATP}, \ldots)$ is representative of ATP synthesis and $C(t, G_{ATP}, \ldots)$ is ATP consumption. Given observed parameters, the energy allocation to a single neuron can be

calculated. Based on experimentally observed values we can estimate this as:

$$\%\text{ neurons in cerebral cortex} \cdot \%\text{ total ATP allocated to brain} (\text{ATP synthesis per cell} \cdot \text{total cells}).$$

Using scaled parameters found in literature, which can be seen in 3.2:

$$\begin{aligned} S(t, G_{ATP}, \ldots) &= \left(\frac{16}{86} \cdot 0.20 \cdot 10^8 \cdot (3.72 \times 10^{13}) \right) t, \\ &= \left(1.384 \times 10^{20} \frac{\text{ATP}}{\text{s}} \right) t. \end{aligned} \tag{3.2}$$

$C(t, G_{ATP}, \ldots)$ includes all neuron energy consumption. This includes the cost of actively firing neurons to spike and the cost of neurons at rest. The cost of actively firing was adopted from "The Cost of Cortical Computation" [35]. Lennie establishes the cost of a single spike in humans to 2.343×10^9 ATP. In seizures the average neuronal firing rate increases by 45.5% [31]. The average human spikes lasts approximately 1 ms. Making the average seizure spike last 0.545 ms. Via unit conversion, spiking costs $4.299 \times 10^{12} \frac{\text{ATP}}{\text{s}}$. The energy costs for neurons at rest is hypothesized to be due to the process of packing neurotransmitters in vesicles [53]. This resting energy consumption is estimated to be $4.7 \times 10^9 \frac{\text{ATP}}{\text{s}}$ [81]. During synaptic inactivity, there is energy leakage from the vesicle membrane creating a proton efflux and correlated energy loss. Based on this,

$$\begin{aligned} C(t, G_{ATP}, \ldots) &= \left(4.299 \times 10^{12} \frac{\text{ATP}}{\text{s}} \right) t + 1.6 \times 10^{10} \left(4.7 \times 10^9 \frac{\text{ATP}}{\text{s}} \right) t, \\ &= \left(7.52 \times 10^{19} \frac{\text{ATP}}{\text{s}} \right) t. \end{aligned} \tag{3.3}$$

Based on equations 3.1 and 3.2, 3.3 can be written as:

$$\begin{aligned}\frac{\mathrm{d}G_{ATP}}{\mathrm{d}t} &= \left(1.384\times10^{20}\frac{\mathrm{ATP}}{\mathrm{s}}\right)t - \left(7.52\times10^{19}\frac{\mathrm{ATP}}{\mathrm{s}}\right)t, \\ &= 6.320\times10^{19}t,\end{aligned} \tag{3.4}$$

where t is a measure of time in seconds.

3.1.2 Network Model

A network model can be adopted from the same framework as the single neuron model. The general form of the differential equation and synthesis equation $S(t, G_{ATP}, \ldots)$ are the same as in the single neuron model.

$$\frac{\mathrm{d}G_{ATP}}{\mathrm{d}t} = S(t, G_{ATP}, \ldots) - C(t, G_{ATP}, \ldots), \tag{3.5}$$

$$S(t, G_{ATP}, \ldots) = 0.44 \cdot .2 \cdot c \cdot c_{ATP} \cdot t. \tag{3.6}$$

$C(t, G_{ATP}, \ldots)$ can be broken down into two main components. There is the energy consumption of seizing neurons and the neurons at rest. Let energy consumption of resting neurons be represented by $\frac{\mathrm{d}r}{\mathrm{d}t}$ such that

$$\frac{\mathrm{d}r}{\mathrm{d}t} = 4.7\times10^{9}. \tag{3.7}$$

For the active seizing neuron, energy is consumed to create and propagate the spike. Additionally, energy is required as an interaction factor for synaptic vesicle release and re-uptake. For a single mm^3 region of cortical neurons, the ATP consumption of a spike

can be calculated via,

$$n_\varepsilon \int_0^t \left(\left| \frac{\mathrm{d}P}{\mathrm{d}t} \right| \right), \tag{3.8}$$

where n_ε is the number of neurons in a mm^3 section of the cerebral cortex.

The energy requirement for neuronal interaction, required for synaptic transmission, is represented as $\frac{\mathrm{d}\psi}{\mathrm{d}t}$, such that,

$$\frac{\mathrm{d}\psi}{\mathrm{d}t} = v_{ATP} f \omega. \tag{3.9}$$

In $\frac{\mathrm{d}\psi}{\mathrm{d}t}$, $v =$ ATP molecules consumed per vesicle released, $f =$ failure rate, and $\omega =$ is the number of synaptic connections per neuron. Related literature suggests there is an decreased rate vesicle fusion failure in epilepsy [73]. Under standard conditions, vesicle failure is measured to be 50% [35]. For the sake of this model this failure rate is estimated to be 40%. Thus,

$$\frac{\mathrm{d}\psi}{\mathrm{d}t} = \left(2.3 \times 10^4 \frac{\text{ATP}}{\text{vesicle release}} \right) (.6)(7{,}000 \text{ synapses}).$$

Making the ATP consumption in firing neurons due to synaptic transmission of $\varepsilon = 1$ mm^3 sections equal to,

$$n_\varepsilon \int_0^t \frac{\mathrm{d}\psi}{\mathrm{d}t}.$$

$C(t, G_{ATP}, ...)$ can be compiled from equations 3.7, 3.8, and 3.9 to be,

$$C(t, G_{ATP}, \ldots) = \varepsilon \left(n_\varepsilon \int_0^t \left(\left| \frac{\mathrm{d}P}{\mathrm{d}t} \right| \right) + n_\varepsilon \int_0^t \left(\frac{\mathrm{d}\psi}{\mathrm{d}t} \right) \right) + (\alpha - \varepsilon) \left(n_\varepsilon \int_0^t \frac{\mathrm{d}r}{\mathrm{d}t} \right). \tag{3.10}$$

Thus, equation 3.5 can be rewritten as the system of equations,

$$\frac{\mathrm{d}G_{ATP}}{\mathrm{d}t} = 0.44 \cdot .2 \cdot c \cdot c_{ATP} \cdot t - \left(\varepsilon \left(n_\varepsilon \int_0^t \left(\mid \frac{\mathrm{d}P}{\mathrm{d}t} \mid \right) + n_\varepsilon \int_0^t \left(\frac{\mathrm{d}\psi}{\mathrm{d}t} \right) \right) + (\alpha - \varepsilon) \left(n_\varepsilon \int_0^t \frac{\mathrm{d}r}{\mathrm{d}t} \right) \right),$$
$$\frac{\mathrm{d}P}{\mathrm{d}t} = |I_{kv}V_k| + |I_{kc}V_K| + |I_lV_l| - |I_iV_i|,$$
$$\frac{\mathrm{d}\psi}{\mathrm{d}t} = 9.66 \times 10^7,$$
$$\frac{\mathrm{d}r}{\mathrm{d}t} = 4.7 \times 10^9, \tag{3.11}$$

where t is a measure of time in seconds, ε is a mm^3 region of firing cortical neurons, α is total volume of the cerebral cortex, and n_ε is the number of neurons in a mm^3 region. I_x and V_x for $x \in \{i, kv, kc, l\}$ are defined by [80]. Key additional parameters are summarized in the table below.

Parameter	Interpretation	Value
g_x, $x \in \{i, kv, kc, l\}$	maximum conductance of respective ion channels	[80]
V_x, $x \in \{i, kv, kc, l\}$	reversal potentials of respective ion channels	[80]
α	total cerebral cortex volume	$\approx 5.03512 \times 10^5 \mathrm{mm}^3$ [1]
ε, $\varepsilon \in [0, \alpha]$	number of mm^3 unit regions seizing	varied
c	number of cells in the human body	3.72×10^{13}
c_{ATP}	total number of ATP molecules synthesized per human cell	varied $\approx 10^8 \frac{\mathrm{ATP}}{\mathrm{ms}}$
n_ε	number of neurons in a mm^3 cortical region	50,000

Table 3.1: Key Model Parameters

3.1.3 Parameters

Scaling a Rat to Human Model

Neurons in the human neocortex are larger than that of a rat and have more synaptic connections. However, their basic organization and structure is not known to differ. Cell body size remains approximately constant at 15 μm in diameter. In scaling a rat brain up to a human brain, its believed that increasing brain size linearly increases cortical thickness, dendrite/axon length and proportionately lowers the density of neurons. An overview of key statistics for the human neurocortex can be seen in 3.2. On the singular synaptic level, they are assumed to be the same in both rat and human neurons.

Table 3.2: Statistics of the Human Brain

Brain Region	Property	Value	Source
Whole Brain	Number of Neurons	86,000,000,000	[24]
	Mass (g)	1508	[24]
	Energy Allocation (%)	20	[54]
Neocortex	Number of Neurons	21	[50]
	Mass (g)		[38]
	Surface Area (mm)	190,000	
	Thickness (mm)	2.5	
	Glucose Consumption	0.40	
	Glia/mm	38,000	
	Neurons/mm	40,000	
	Synapses/mm	7 x 10^{8}	
	Average Axon Length m/mm	4,000	
	Dendrite Length m/mm	400	
	Average Dendrite Diameter	0.9	
Cerebral Cortex	Number of Neurons	16,000,000,000	[74]
	Mass (g)	1233	[24]
Cerebellum	Number of Neurons	69,000,000,000	[24]
	Mass (g)	154	
Cell	ATP Production $\left(\frac{\text{ATP}}{\text{s}}\right)$	10^7	[17]

Scaling Normal Parameters to Seizure State

Changes in membrane voltage brought about by ion fluxes are the foundation to single neuron activity. Electrochemical gradients drive the flow of ions, directly effecting other critical features such as synaptic transmission and signal propagation. During an epileptic seizure these activities become severely perturbed. This deviation from normal electrochemical signaling had to be incorporated mathematically into the normal bursting model.

Reversal Potential

Reversal potential is a function of the transmembrane concentration gradients. In patients with epilepsy experiments using ion specific electrodes demonstrated altered baseline extra- and intra- cellular concentrations. There was a particularly large shift (25-fold decrease) in baseline extracellular K^+ concentration which consequently created a relatively large increase in the reversal potential for K^+ from approximately -85mV to -55 mV [55]. In addition, in vivo experiments observed a dissipation of transmembrane Ca^{2+} which would cause a negative shift in reversal potentials. This shift was estimated to alter the reversal potential from 137 mV to 66 mV [36]. Due to these two changes, there is likely also a corresponding shift in Na^+, Cl^-, and HCO_3^+ reversal potentials estimated to be 25 mV, -47 mV, and -25 mV respectively [55].

Channel Conductance

Channel conductance constants can be calculated via $g = G_{max}O$ where G_{max} is the maximum channel conductance and O is the probability that the channel is open. In epilepsy, exome sequencing identified minor gain-of-function variants [43]. However, these findings are controversial and small in magnitude. Thus, largely the channel con-

ductance parameters do not need to be adjusted.

Synaptic Activity

In epilepsy the release probability and re-uptake probability increase [73]. Thus, the failure rate decreases.

3.1.4 Assumptions

Several key assumptions are needed for the validity of the model and to make subsequent conclusions about energy limitations. First, in order to build the model, assumptions had to be made regarding some similarities between mouse and human neuro-anatomy. The most important of which is that human circuitry and network dynamics are linearly scaled from mouse circuitry [3]. This allowed for the derivation of certain parameters that have been yet to be measured in the human brain. Recognizing the variation among parameters and seizure presentations amongst age groups, this model is limited to represent adults. Furthermore, in order to make any assumptions about energy limitations, the model is limited to represent only convulsive seizures. In the absence of this assumption, the brain could simply pull energy from other regions of the body. Due to limitations in current methods of measuring and observing neuronal activity, this model also only accounts for cortical behaviors.

In order to scale the model to a network, it is assumed that neurons fire concurrently in excitatory patterns with synchrony. Although a simplification of realistic biological systems, it is plausible to make these simplifying assumptions due to the nature of seizure dynamics. Recurrent epileptic seizures have been shown to have pathological synchronous behavior of neurons. Via electrocardiogram imaging, patients during epileptic seizures

exhibited a increase in synchronization during the seizure, with the maximal synchronization immediately before seizure termination [38]. Additionally, the volume of 1 mm^3 of neuronal region was selected for ε due to the propagation of seizures occurring in both transverse and longitudinal directions [57].

Chapter 4

Results

4.1 Single Neuron Model

For a single neuron model, the membrane potential (voltage over time) phase portraits were established for a single burst, and adopted to epileptic parameters found in literature. This (Figure 4.1) was compared to a multi-burst phase portrait of a normal neuron.

This enabled a comparative analysis of power phase planes. Under seizure conditions, with adapted parameters, power continuously increased and within the first millisecond of spiking increases exponentially. To derive ATP consumption from Figure 4.1 and 4.4, the integral or the area under of the curve was calculated. In seizing state, the area under the curve continually grows substantially compared to normal bursting.

However, despite the expensive energy cost, a seizing neuron can be preserved for a long period of time. In theory, a single bursting neuron could fire infinitely. Given the model:

$$\frac{\mathrm{d}G_{ATP}}{\mathrm{d}t} = 1.384 \times 10^{20} t - 7.52 \times 10^{19} t, \tag{4.1}$$

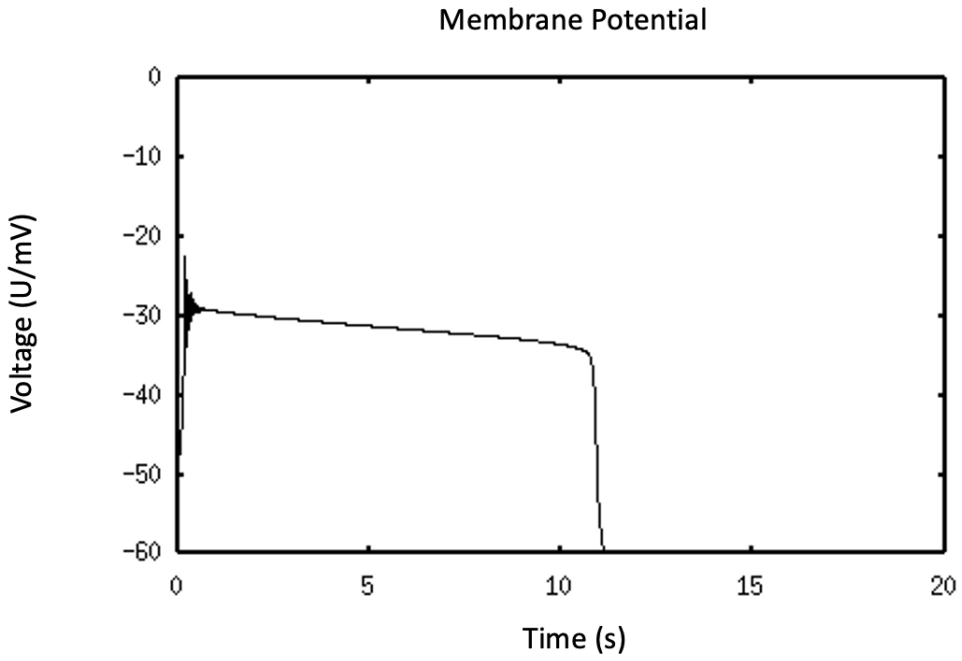

Figure 4.1: A single burst voltage over time phase plane for a bursting Chay model neuron with $V_i = 100$, $V_k = -75$, $V_l = -40$, $V_c = 100$, $g_i = 1800$, $g_k v = 1700$, $g_k c = 11.5$, $g_l = 7$, $k_c = 0.03$, $\rho = 0.27$, $\lambda = 400$, $g_k = 37$

$$\begin{aligned} \lim_{t\to\infty}\left(\frac{\mathrm{d}G_{ATP}}{\mathrm{d}t} = 1.384\times10^{20}t - 7.52\times10^{19}t\right), \\ = 10^{20}\cdot t - 10^{19}\cdot t, \\ = \infty. \end{aligned} \tag{4.2}$$

The energy supply continually accumulates, creating the necessary stores for a neuron to continuing firing despite its consumption.

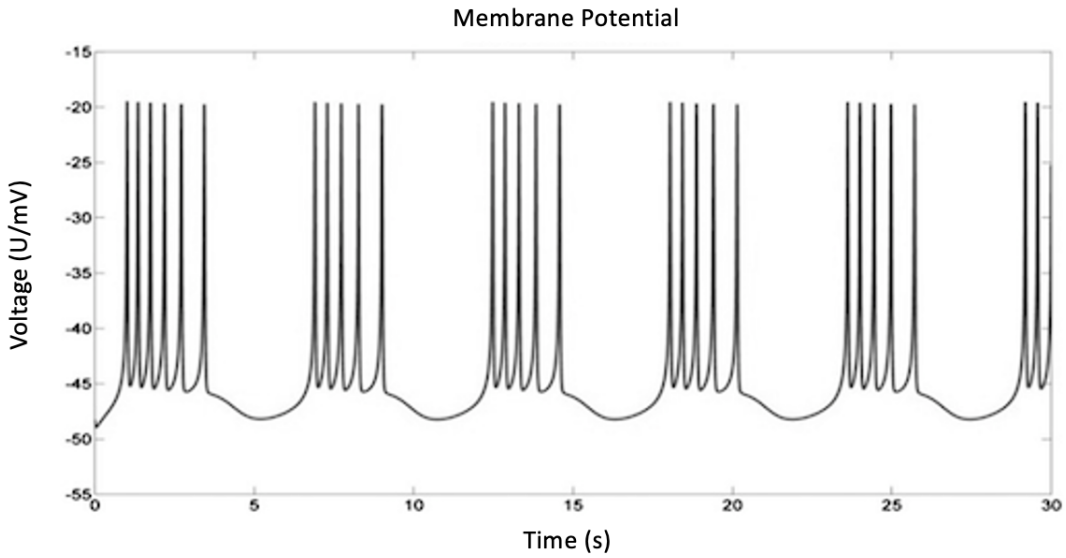

Figure 4.2: A multi-burst firing simulated by the Chay model ($V_i = 100$ mV, $V_k = 75$ mV, $V_l = -40$ mV, $V_c = 100$ mV, $g_i = 1800$ nS, $g_{kv} = 1700$ nS, $g_{kc} = 11.5$ nS, and $g_l = 7$ nS).

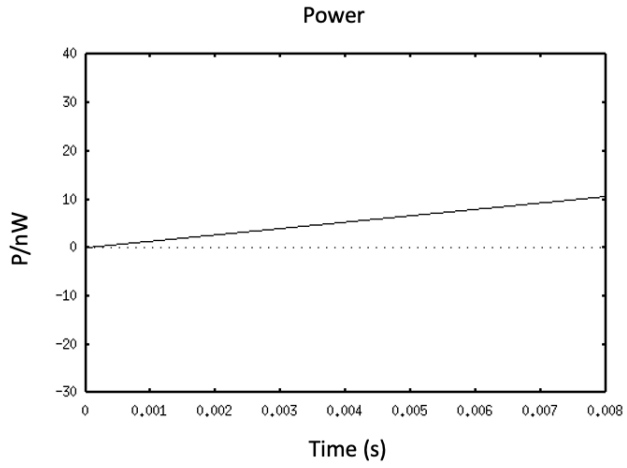

Figure 4.3: This is the graph of the energy corresponding to the spike diagram 4.1. The power phase plane shows continuous energy absorption in a seizing state. As a single burst, this diagram does not account for the energy needed to recover to resting potential.

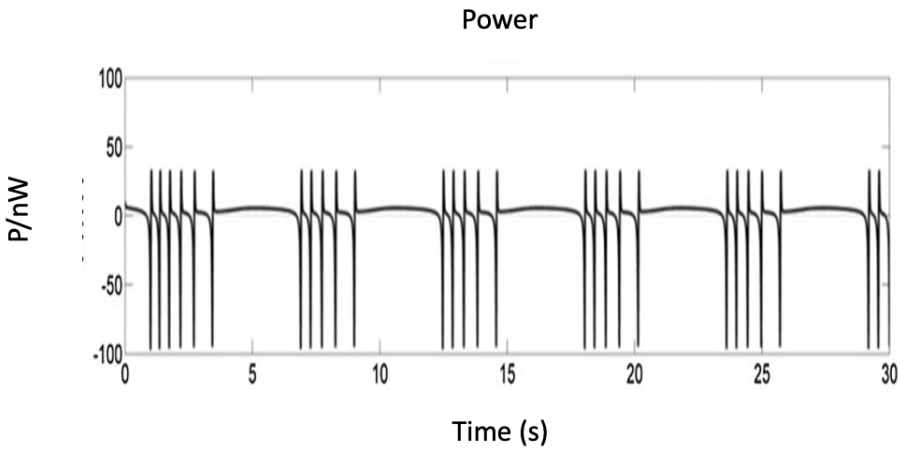

Figure 4.4: This is the graph of the energy corresponding to the spike diagram . P is an alternation between electrical energy release and absorption. Between bursts the neuron requires longer energy to recover to resting potential. Parameters correspond to those in 4.2

4.2 Neural Network Model

In its entirety, the neural network model is governed by the following system of equations

$$\frac{\mathrm{d}G_{ATP}}{\mathrm{d}t} = 0.088c \times t \times c_{ATP} - \left(\varepsilon n_\varepsilon \int_0^t \left(\mid \frac{\mathrm{d}P}{\mathrm{d}t} \mid + \frac{\mathrm{d}\psi}{\mathrm{d}t} \right) + (\alpha - \varepsilon) n_\varepsilon \int_0^t \frac{\mathrm{d}r}{\mathrm{d}t} \right),$$

$$\frac{\mathrm{d}P}{\mathrm{d}t} = \mid I_{kv}V_k \mid + \mid I_{kc}V_K \mid + \mid I_l V_l \mid - \mid I_i V_i \mid,$$

$$\frac{\mathrm{d}\psi}{\mathrm{d}t} = 9.66 \times 10^7,$$

$$\frac{\mathrm{d}r}{\mathrm{d}t} = 4.7 \times 10^9.$$

From the Chay Model:

$$\frac{dn}{dt} = \frac{n_\infty - n}{\tau_n},$$
$$\frac{dC}{dt} = \rho\left(m_\infty^3 h_\infty (V_c - V) - k_c C\right),$$
$$\frac{dV}{dt} = g_i M_\infty^3 h_\infty (V_i - V) + g_{kc} n^4 (V_k - V) + g_{kc}\frac{C}{1+C}(V_k - V) + g_l(V_l - V) + I,$$

$$m_\infty = \frac{2.5 + .1V}{2.5 + .1V + (4e^{-(V+50)/18})(1 - e^{-.1V-25})},$$
$$h_\infty = \frac{(.07e^{-.05V-2.5})(1 + e^{-0.1V-2})}{(.07e^{-.05V-2.5})(1 + e^{-.1V-2}) + 1},$$
$$n_\infty = \frac{.01V + .2}{(1 - e^{-.1V-2})(.125e^{-(V+30)/80} + .01V + .2)},$$
$$\tau_n = \frac{1}{\lambda_n(.7e^{-.05V-2.5})(\frac{1}{1+e^{-.1V-2}})}.$$

The network model yields three plausible conditions, each dictating discrete seizure events.

1. $\frac{dG_{ATP}}{dt} < 0$: indicating that, $0 > S(t, G_{ATP}, \ldots) - C(t, G_{ATP}, \ldots)$. In order for this to be true it follows that,

$$S(t, G_{ATP}, \ldots) < C(t, G_{ATP}, \ldots). \tag{4.3}$$

   In this case, the neuronal behavior is consuming energy at a greater rate than it is produced. As a result, there are insufficient resources for firing to continue at the existing rate and spatial scale.

2. $\frac{dG_{ATP}}{dt} = 0$: indicating that, $0 = S(t, G_{ATP}, \ldots) - C(t, G_{ATP}, \ldots)$. In order for this to

be true it follows that,

$$S(t, G_{ATP}, \ldots) = C(t, G_{ATP}, \ldots). \tag{4.4}$$

This is an equilibrium state. In these conditions, the rate at which ATP is being consumed is equal to the rate at which it is being produced. This means a seizure can sustain existing dynamics. However, the system does not have the resources to scale neuronal behavior either via increasing firing rates or the number of firing neurons.

3. $\frac{dG_{ATP}}{dt} > 0$: indicating that, $0 < S(t, G_{ATP}, \ldots) - C(t, G_{ATP}, \ldots)$. In order for this to be true it follows that,

$$S(t, G_{ATP}, \ldots) > C(t, G_{ATP}, \ldots). \tag{4.5}$$

Under these conditions, there is an energy surplus. This means some energy that is produced, and that is traditionally allocated to the brain, is not being used. This energy may either be stored or reallocated to alternative function. The excess energy indicates the rate of neuronal firing could be increased or the seizure could further propagate to a larger region of the brain.

4.2.1 Maximum Seizing Volume Calculations

The maximum volume of cortical region that could sustain seizing dynamics for time t was calculated for two seizure dynamics based on energy availability.

Maxi-Min Approximation

The maximum constraints can be approximated by inserting Lennie's calculated cost of a single spike, the average firing frequency, and seizure time into the established model. Lennie estimates the cost of a single spike to be, 2.4×10^9 molecules of ATP [35]. As stated earlier, the average seizure spike last approximately .545 ms. This indicates spiking alone will cost 4.404×10^{12} molecules of ATP per second.

$$\begin{aligned}
\frac{\mathrm{d}G_{ATP}}{\mathrm{d}t} &= 0.0880c \times t \times c_{ATP} - \left(\varepsilon n_\varepsilon \int_0^t \left(4.404 \times 10^{12} + \frac{\mathrm{d}\psi}{\mathrm{d}t}\right) + (\alpha - \varepsilon) n_\varepsilon \int_0^t \frac{\mathrm{d}r}{\mathrm{d}t}\right), \\
&= 3.274 \times 10^{20} t - \left(\varepsilon n_\varepsilon \left(4.404 \times 10^{12} t + 9.660 \times 10^{7} t\right) + (\alpha - \varepsilon) n_\varepsilon 4.700 \times 10^{9} t\right), \\
&= 3.274 \times 10^{20} t - \left(\varepsilon \left(2.202 \times 10^{17} t + 4.830 \times 10^{12} t\right) + (\alpha - \varepsilon) 2.350 \times 10^{14} t\right), \\
&= 3.274 \times 10^{20} t - \left(\varepsilon \left(2.202 \times 10^{17} t\right) + (2.350 \times 10^{14} t\alpha - 2.350 \times 10^{14} t\varepsilon)\right), \\
&= 3.274 \times 10^{20} t - 2.200 \times 10^{17} t\varepsilon - 1.183 \times 10^{20} t, \\
&= 2.0903 \times 10^{20} t - 2.200 \times 10^{17} t\varepsilon.
\end{aligned}$$

At equilibrium the equation above simplifies to $2.090 \times 10^{20} t = 2.200 \times 10^{17} t\varepsilon$. Thus, regardless of time duration t, there is a steady state when $\varepsilon = 950.3\text{mm}^3$ or 95.03cm^3 . Following the three states established earlier:

1. $\frac{\mathrm{d}G_{ATP}}{\mathrm{d}t} < 0$ when $\varepsilon > 950.3\text{mm}^3$ indicating the seizure runs out of energy,
2. $\frac{\mathrm{d}G_{ATP}}{\mathrm{d}t} = 0$ when $\varepsilon = 950.3\text{mm}^3$ indicating the seizure can not grow and,
3. $\frac{\mathrm{d}G_{ATP}}{\mathrm{d}t} > 0$ when $\varepsilon < 950.3\text{mm}^3$ indicating there is excess energy.

Model Estimation

The power component to the generalized model was solved using MATLAB's ODE45 algorithms where the starting conditions $(V_{init}, n_{init}, C_{init})$ of 1 mV, 0.1, 0.1 nmol/L are fixed. Unlike in the maxi-min approximation, here the t value will effect the calculation since P is a non-linear function of time.

$$\frac{\mathrm{d}G_{ATP}}{\mathrm{d}t} = 0.088c \times t \times c_{ATP} - \left(\varepsilon n_{\varepsilon} \int_0^t \left(|\frac{\mathrm{d}P}{\mathrm{d}t}| + \frac{\mathrm{d}\psi}{\mathrm{d}t}\right) + (\alpha - \varepsilon) n_{\varepsilon} \int_0^t \frac{\mathrm{d}r}{\mathrm{d}t}\right).$$

Simplifying all of the parameters

$$\frac{\mathrm{d}G_{ATP}}{\mathrm{d}t} = -2.0903 \times 10^{20} t + 50000\varepsilon \int_0^t |\frac{\mathrm{d}P}{\mathrm{d}t}| - 2.3017 \times 10^{14} t\varepsilon.$$

Energy constraints were first calculated for a complex partial seizure. The average duration of a complex partial seizure is between 30 and 120 seconds. Thus, to represent a complex partial seizure t is estimated to be equal to 75.5 seconds. In setting $t = 75.5$,

$$\begin{aligned}\frac{\mathrm{d}G_{ATP}}{\mathrm{d}t} &= -2.0903 \times 10^{20}(75.7) + 50000\varepsilon \int_0^{75.5} |\frac{\mathrm{d}P}{\mathrm{d}t}| - 2.3017 \times 10^{14}(75.5)\varepsilon, \\ &= -1.5824 \times 10^{22} + 50000\varepsilon \int_0^{75.5} |\frac{\mathrm{d}P}{\mathrm{d}t}| - 1.7424 \times 10^{16}\varepsilon.\end{aligned}$$

From MATLAB's ODE45 program $\int_0^{75.5} |\frac{\mathrm{d}P}{\mathrm{d}t}| \approx 10^{13}$. Thus,

$$\begin{aligned}\frac{\mathrm{d}G_{ATP}}{\mathrm{d}t} &= -1.5824 \times 10^{22} + 5 \times 10^{17}\varepsilon - 1.7424 \times 10^{16}\varepsilon, \\ &= -1.5824 \times 10^{22} + 3.258 \times 10^{17}\varepsilon,\end{aligned} \tag{4.6}$$

where $\varepsilon = \text{mm}^3$ volume of seizing neurons. Establishing the conditions from Section 4.2,

1. $\dfrac{\mathrm{d}G_{ATP}}{\mathrm{d}t} < 0$ when $\varepsilon > 32790.69\ \text{mm}^3$,
2. $\dfrac{\mathrm{d}G_{ATP}}{\mathrm{d}t} = 0$ when $\varepsilon = 32790.69\ \text{mm}^3$,
3. $\dfrac{\mathrm{d}G_{ATP}}{\mathrm{d}t} > 0$ when $\varepsilon < 32790.69\ \text{mm}^3$.

As a function of ε and t, with knowledge of the volume of seizing neurons, one could calculate time t that the seizure could last from the model as well.

Chapter 5

Discussion

The proposed model provides insight on the role of energy in mediating seizure termination. It validates the hypothesis that energy can act as a limiting reagent. An individual neuron was seen to be rather computationally expensive, however energy will only cause termination in seizures characterized by wide-spread neuronal hyper-activity. This indicates there may be another additional factor besides energy mediating seizure termination. These results are consistent with experimental studies which observed on average simple partial seizures had the longest duration while generalized tonic-clonic seizures lasted the shortest. Mathematically, it illustrates how a small focal seizure in the lip can last for days, while a tonic-clonic seizure effecting both hemispheres of the brain will likely not last more than a few hundred seconds.

Calculated results re-open a long standing debate regarding the implications of a single spike-wave discharge on cortical energy management. In prior literature, it was estimated that $10-20\text{cm}^2$ of cortex was necessary to generate a single spike-wave discharge, making the generation of a single spike-wave discharge the activity of 10^8 neurons [47] [48].

However, the research proposed in this paper argues that a single-spike wave discharge has significant implications to all cortical energy management, which is traditionally only seen as a signature of an epileptic focus. In the maximum estimation case, there is barely enough energy to form a single spike wave. The model estimates approximately $20.82 cm^2$ to be the maximum amount power consumption, due to hyper-active neuronal spikes, that the brain can support. This re-introduces a phenomenon prior urged by pediatric neurologists towards aggressively treating even a single spike-wave discharge in children.

Increased knowledge of seizure termination mechanisms will undoubtedly have critical implications for the development of anti-seizure therapies. Seizure termination is incredibly difficult to study experimentally since the manipulation of potential terminating mechanisms will also likely directly manipulate traits responsible for seizure initiation and propagation. Also during a post-ictal phase, complex mechanisms effect each other in non-isolatable complex ways. Thus, models like the one established in this paper, provide critical insight into plausible mechanisms.

Although the present results suggest that energy plays a role in seizure termination mechanisms, it is impossible to definitively make this statement without further validation through in vivo experiments and more advanced modeling. As stated earlier, there were several key assumptions underlying the model. Most notably, the model simplifies neurons to a point mechanism with the absence of a time delay. Due to the lack of research and definitive data, many of the parameters also had to be estimated. With further research there is hope to provide a more exact model of these dynamics. Furthermore, the model does not account for many complex interactions that occur during seizures and in neural control. Further research using PET scan analysis in post-ictal states may shed light on the lack of precise knowledge of seizure state ionic, metabolic, and synaptic behavior. Despite

these limitations, this research can be seen as a key step towards integrating mathematical modeling and metabolic processes to enhance our understanding of seizure termination mechanisms.

Bibliography

[1] Munjal M Acharya and Surendra S Katyare. Structural and functional alterations in mitochondrial membrane in picrotoxin-induced epileptic rat brain. *Experimental Neurology*, 192(1):79–88, 2005.

[2] David Attwell and Simon B Laughlin. An energy budget for signaling in the grey matter of the brain. *Journal of Cerebral Blood Flow & Metabolism*, 21(10):1133–1145, 2001.

[3] Frederico AC Azevedo, Ludmila RB Carvalho, Lea T Grinberg, José Marcelo Farfel, Renata EL Ferretti, Renata EP Leite, Wilson Jacob Filho, Roberto Lent, and Suzana Herculano-Houzel. Equal numbers of neuronal and nonneuronal cells make the human brain an isometrically scaled-up primate brain. *Journal of Comparative Neurology*, 513(5):532–541, 2009.

[4] Gerold Baier and John Milton. Dynamic diseases of the brain., 2014.

[5] Paolo Bazzigaluppi, Azin Ebrahim Amini, Iliya Weisspapir, Bojana Stefanovic, and Peter L Carlen. Hungry neurons: metabolic insights on seizure dynamics. *International Journal of Molecular Sciences*, 18(11):2269, 2017.

[6] Ettore Beghi. The epidemiology of epilepsy. *Neuroepidemiology*, 54(2):185–191, 2020.

[7] Ettore Beghi and Giorgia Giussani. Aging and the epidemiology of epilepsy. *Neuroepidemiology*, 51(3-4):216–223, 2018.

[8] HF Bradford. Glutamate, gaba and epilepsy. *Progress in neurobiology*, 47(6):477–511, 1995.

[9] Teresa Ree Chay. Chaos in a three-variable model of an excitable cell. *Physica D: Nonlinear Phenomena*, 16(2):233–242, 1985.

[10] Ben A Chindo, Bulus Adzu, and Karniyus S Gamaniel. Antiepileptic drug targets: An update on ion channels. *Epileptology—The Modern State of Science*, 2016.

[11] PJ Cohen, SC Alexander, Th C Smith, MARTIN Reivich, and HARRY Wollman. Effects of hypoxia and normocarbia on cerebral blood flow and metabolism in conscious man. *Journal of Applied Physiology*, 23(2):183–189, 1967.

[12] Kiranjit K Dhillon and Sonu Gupta. Biochemistry, ketogenesis. In *StatPearls [Internet]*. StatPearls Publishing, 2021.

[13] Kenza El Houssaini, Christophe Bernard, and Viktor K Jirsa. The epileptor model: a systematic mathematical analysis linked to the dynamics of seizures, refractory status epilepticus, and depolarization block. *Eneuro*, 7(2), 2020.

[14] Jerome Engel. Pet scanning in partial epilepsy. *Canadian journal of neurological sciences*, 18(S4):588–592, 1991.

[15] Yanqing Fei, Ruting Shi, Zhi Song, and Jinze Wu. Metabolic control of epilepsy: a promising therapeutic target for epilepsy. *Frontiers in Neurology*, 11:1694, 2020.

[16] Kirsten M Fiest, Khara M Sauro, Samuel Wiebe, Scott B Patten, Churl-Su Kwon, Jonathan Dykeman, Tamara Pringsheim, Diane L Lorenzetti, and Nathalie Jetté. Prevalence and incidence of epilepsy: a systematic review and meta-analysis of international studies. *Neurology*, 88(3):296–303, 2017.

[17] Avi Flamholz, Rob Phillips, and Ron Milo. The quantified cell. *Molecular biology of the cell*, 25(22):3497–3500, 2014.

[18] Jaroslava Folbergrová, Pavel Ješina, Zdeněk Drahota, Václav Lisỳ, Renata Haugvicová, Alena Vojtíšková, and Josef Houštěk. Mitochondrial complex i inhibition in cerebral cortex of immature rats following homocysteic acid-induced seizures. *Experimental neurology*, 204(2):597–609, 2007.

[19] Leon Glass and Michael Mackey. Mackey-glass equation. *Scholarpedia*, 5(3):6908, 2010.

[20] Adam L Hartman, Maciej Gasior, Eileen PG Vining, and Michael A Rogawski. The neuropharmacology of the ketogenic diet. *Pediatric neurology*, 36(5):281–292, 2007.

[21] W Allen Hauser. Seizure disorders: the changes with age. *Epilepsia*, 33:6–14, 1992.

[22] W Allen Hauser, John F Annegers, and Lila R Elveback. Mortality in patients with epilepsy. *Epilepsia*, 21(4):399–412, 1980.

[23] Sandra L Helmers, David J Thurman, Tracy L Durgin, Akshatha Kalsanka Pai, and Edward Faught. Descriptive epidemiology of epilepsy in the us population: a different approach. *Epilepsia*, 56(6):942–948, 2015.

[24] Suzana Herculano-Houzel. The human brain in numbers: a linearly scaled-up primate brain. *Frontiers in human neuroscience*, page 31, 2009.

[25] Nikolas Hitiris, Rajiv Mohanraj, John Norrie, and Martin J Brodie. Mortality in epilepsy. *Epilepsy & behavior*, 10(3):363–376, 2007.

[26] Washington University in St. Louis. Fast-slow dynamical systems.

[27] Eugene M Izhikevich. *Dynamical systems in neuroscience*. MIT press, 2007.

[28] Eugene M Izhikevich. Hybrid spiking models. *Philosophical Transactions of the Royal Society A: Mathematical, Physical and Engineering Sciences*, 368(1930):5061–5070, 2010.

[29] John Hughlings Jackson. Note on the comparison and contrast of regional palsy and spasm. *The Lancet*, 89(2271):295–297, 1867.

[30] Viktor K Jirsa, William C Stacey, Pascale P Quilichini, Anton I Ivanov, and Christophe Bernard. On the nature of seizure dynamics. *Brain*, 137(8):2210–2230, 2014.

[31] Barbara C Jobst. What is a seizure? insights from human single-neuron recordings: What is a seizure? *Epilepsy Currents*, 12(4):135–137, 2012.

[32] Arthur Kreindler. Experimental epilepsy. 1965.

[33] Fred A Lado and Solomon L Moshé. How do seizures stop? *Epilepsia*, 49(10):1651–1664, 2008.

[34] Anthony T Lee, John F Burke, Pranathi Chunduru, Annette M Molinaro, Robert Knowlton, and Edward F Chang. A historical cohort of temporal lobe surgery for medically refractory epilepsy: a systematic review and meta-analysis to guide future nonrandomized controlled trial studies. *Journal of neurosurgery*, 133(1):71–78, 2019.

[35] Peter Lennie. The cost of cortical computation. *Current biology*, 13(6):493–497, 2003.

[36] Florian Lesage. Pharmacology of neuronal background potassium channels. *Neuropharmacology*, 44(1):1–7, 2003.

[37] Ho Ling Li and Mark Cw Van Rossum. Energy efficient synaptic plasticity. *Elife*, 9:e50804, 2020.

[38] Jan H Lui, David V Hansen, and Arnold R Kriegstein. Development and evolution of the human neocortex. *Cell*, 146(1):18–36, 2011.

[39] Frederic Mery and Tadeusz J Kawecki. A cost of long-term memory in drosophila. *Science*, 308(5725):1148–1148, 2005.

[40] John Milton. *Epilepsy as a dynamic disease*. Springer Science & Business Media, 2003.

[41] Karl O Nakken, Kjell Heuser, Kristin Alfstad, and Erik Taubøll. How do antiepileptic drugs work? *Tidsskrift for den Norske laegeforening: Tidsskrift for praktisk medicin, ny raekke*, 134(1):42–46, 2014.

[42] Ronald Neppl, Canh M Nguyen, William Bowen, Taoufik Al-Saadi, Jeanne Pallagi, George Morris, Wade Mueller, Roger Johnson, Robert Prost, and Scott D Rand. In vivo detection of postictal perturbations of cerebral metabolism by use of proton mr spectroscopy: preliminary results in a canine model of prolonged generalized seizures. *American journal of neuroradiology*, 22(10):1933–1943, 2001.

[43] Zachary Niday and Anastasios V Tzingounis. Potassium channel gain of function in epilepsy: an unresolved paradox. *The Neuroscientist*, 24(4):368–380, 2018.

[44] University of Bristol. Brain imaging.

[45] Toru Ohira and John Milton. *Mathematics As a Laboratory Tool: Dynamics, Delays and Noise*. Springer, 2021.

[46] World Health Organization, Global Campaign against Epilepsy, Programme for Neurological Diseases, Neuroscience (World Health Organization), International Bureau for Epilepsy, World Health Organization. Department of Mental Health, Substance Abuse, International Bureau of Epilepsy, and International League against Epilepsy. *Atlas: epilepsy care in the world*. World Health Organization, 2005.

[47] Ivan Osorio, Mark G Frei, Didier Sornette, and John Milton. Pharmaco-resistant seizures: self-triggering capacity, scale-free properties and predictability? *European Journal of Neuroscience*, 30(8):1554–1558, 2009.

[48] Ivan Osorio, Mark G Frei, Didier Sornette, John Milton, and Ying-Cheng Lai. Epileptic seizures: Quakes of the brain? *Physical Review E*, 82(2):021919, 2010.

[49] Ruth Ottman, Richard B Lipton, Alan B Ettinger, Joyce A Cramer, Michael L Reed, Alan Morrison, and George J Wan. Comorbidities of epilepsy: results from the epilepsy comorbidities and health (epic) survey. *Epilepsia*, 52(2):308–315, 2011.

[50] Bente Pakkenberg and Hans Jørgen G Gundersen. Neocortical neuron number in humans: effect of sex and age. *Journal of comparative neurology*, 384(2):312–320, 1997.

[51] Emilio Perucca. An introduction to antiepileptic drugs. *Epilepsia*, 46:31–37, 2005.

[52] David A Prince. Neurophysiology of epilepsy. *Annual review of neuroscience*, 1(1):395–415, 1978.

[53] Camila Pulido and Timothy A Ryan. Synaptic vesicle pools are a major hidden resting metabolic burden of nerve terminals. *Science advances*, 7(49):eabi9027, 2021.

[54] Marcus E Raichle and Debra A Gusnard. Appraising the brain's energy budget. *Proceedings of the National Academy of Sciences*, 99(16):10237–10239, 2002.

[55] Joseph V Raimondo, Richard J Burman, Arieh A Katz, and Colin J Akerman. Ion dynamics during seizures. *Frontiers in cellular neuroscience*, 9:419, 2015.

[56] Doodipala Samba Reddy. Role of hormones and neurosteroids in epileptogenesis. *Frontiers in cellular neuroscience*, 7:115, 2013.

[57] Xin Ren. *Dynamic Emergence of Neuronal Synchrony during Kindling*. PhD thesis, University of Virginia, 2013.

[58] Blake A Richards and Paul W Frankland. The persistence and transience of memory. *Neuron*, 94(6):1071–1084, 2017.

[59] Leone Ridsdale, Judith Charlton, Mark Ashworth, Mark P Richardson, and Martin C Gulliford. Epilepsy mortality and risk factors for death in epilepsy: a population-based study. *British Journal of General Practice*, 61(586):e271–e278, 2011.

[60] Michael A Rogawski and Wolfgang Löscher. The neurobiology of antiepileptic drugs. *Nature reviews neuroscience*, 5(7):553–564, 2004.

[61] Maria Luisa Saggio, Dakota Crisp, Jared M Scott, Philippa Karoly, Levin Kuhlmann, Mitsuyoshi Nakatani, Tomohiko Murai, Matthias Dümpelmann, Andreas Schulze-Bonhage, Akio Ikeda, et al. A taxonomy of seizure dynamotypes. *Elife*, 9:e55632, 2020.

[62] Josemir W Sander. The epidemiology of epilepsy revisited. *Current opinion in neurology*, 16(2):165–170, 2003.

[63] Neil Savage. Epidemiology: The complexities of epilepsy. *Nature*, 511(7508):S2–S3, 2014.

[64] Ivanka Savic, Lori Altshuler, Lew Baxter, and Jerome Engel. Pattern of interictal hypometabolism in pet scans with fludeoxyglucose f 18 reflects prior seizure types in patients with mesial temporal lobe seizures. *Archives of neurology*, 54(2):129–136, 1997.

[65] Michael Seidenberg, Dalin T Pulsipher, and Bruce Hermann. Association of epilepsy and comorbid conditions. *Future neurology*, 4(5):663–668, 2009.

[66] Simon D Shorvon. The epidemiology and treatment of chronic and refractory epilepsy. *Epilepsia*, 37:S1–S3, 1996.

[67] Simon D Shorvon. The etiologic classification of epilepsy. *Epilepsia*, 52(6):1052–1057, 2011.

[68] Günther Sperk, Sabine Furtinger, Christoph Schwarzer, and Susanne Pirker. Gaba and its receptors in epilepsy. *Recent advances in epilepsy research*, pages 92–103, 2004.

[69] Carl E Stafstrom and Jong M Rho. *Epilepsy and the ketogenic diet*. Springer Science & Business Media, 2004.

[70] Roxana A Stefanescu, RG Shivakeshavan, and Sachin S Talathi. Computational models of epilepsy. *Seizure*, 21(10):748–759, 2012.

[71] William H Theodore and Robert S Fisher. Brain stimulation for epilepsy. *The Lancet Neurology*, 3(2):111–118, 2004.

[72] Roland D Thijs, Rainer Surges, Terence J O'Brien, and Josemir W Sander. Epilepsy in adults. *The Lancet*, 393(10172):689–701, 2019.

[73] Chirag Upreti, Rafael Otero, Carlos Partida, Frank Skinner, Ravi Thakker, Luis F Pacheco, Zhen-yu Zhou, Giorgi Maglakelidze, Jana Velíšková, Libor Velíšek, et al. Altered neurotransmitter release, vesicle recycling and presynaptic structure in the pilocarpine model of temporal lobe epilepsy. *Brain*, 135(3):869–885, 2012.

[74] David C Van Essen, Chad J Donahue, and Matthew F Glasser. Development and evolution of cerebral and cerebellar cortex. *Brain, behavior and evolution*, 91:158–169, 2018.

[75] Gerben van Hameren, Graham Campbell, Marie Deck, Jade Berthelot, Benoit Gautier, Patrice Quintana, Roman Chrast, and Nicolas Tricaud. In vivo real-time dynamics of atp and ros production in axonal mitochondria show decoupling in mouse models of peripheral neuropathies. *Acta neuropathologica communications*, 7(1):1–16, 2019.

[76] Rodrigo C Vergara, Sebastián Jaramillo-Riveri, Alejandro Luarte, Cristóbal Moënne-Loccoz, Rómulo Fuentes, Andrés Couve, and Pedro E Maldonado. The energy homeostasis principle: neuronal energy regulation drives local network dynamics generating behavior. *Frontiers in computational neuroscience*, page 49, 2019.

[77] Yi Wang and Zhong Chen. An update for epilepsy research and antiepileptic drug development: Toward precise circuit therapy. *Pharmacology & therapeutics*, 201:77–93, 2019.

[78] Claude G Wasterlain, Denson G Fujikawa, LaRoy Penix, and Raman Sankar. Pathophysiological mechanisms of brain damage from status epilepticus. *Epilepsia*, 34:S37–S53, 1993.

[79] Heng Yang, Jiongxing Wu, Ren Guo, Yufen Peng, Wen Zheng, Ding Liu, and Zhi Song. Glycolysis in energy metabolism during seizures. *Neural regeneration research*, 8(14):1316, 2013.

[80] Fengyun Zhu, Rubin Wang, Xiaochuan Pan, and Zhenyu Zhu. Energy expenditure computation of a single bursting neuron. *Cognitive Neurodynamics*, 13(1):75–87, 2019.

[81] Xiao-Hong Zhu, Hongyan Qiao, Fei Du, Qiang Xiong, Xiao Liu, Xiaoliang Zhang, Kamil Ugurbil, and Wei Chen. Quantitative imaging of energy expenditure in human brain. *Neuroimage*, 60(4):2107–2117, 2012.

[82] Frédéric Zubler, Andreas Steimer, Heidemarie Gast, and Kaspar A Schindler. Seizure termination. *International Review of Neurobiology*, 114:187–207, 2014.

Appendix A

Normal and Seizure State PET Scan Comparison

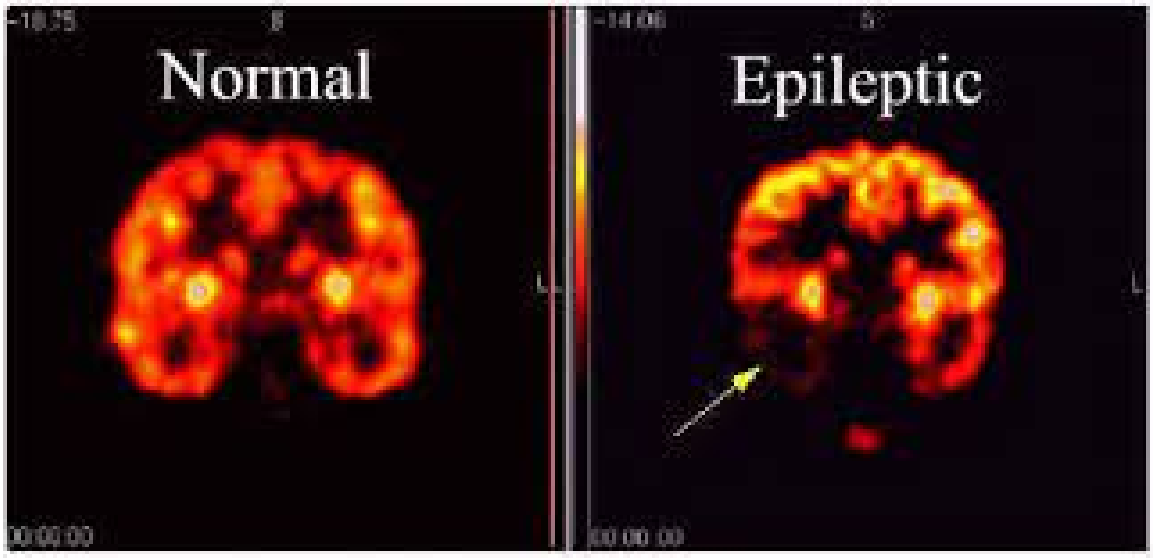

Figure A.1: PET imaging in normal and epileptic brain [44].

Appendix B

Ionic Channel Circuitry Schematic Diagram

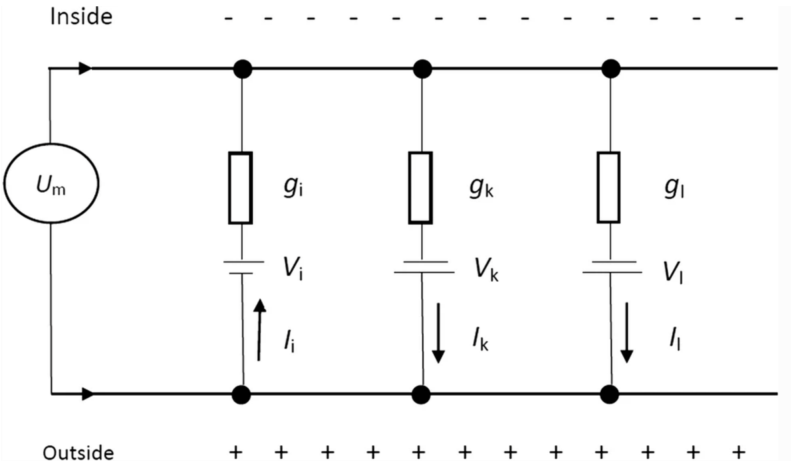

Figure B.1: Schematic diagram of an electrical circuit model of the neural membrane, whose properties establish the foundation for the power function. Voltage sources (V_i, V_k, V_l) correspond to reversal potentials and (I_i, I_k, I_l) correspond to voltage sources [80].

Appendix C

XPP Code For Chay Model

```
# EQUATIONS

dv/dt = gi*m(v)^3*h(v)*(vi - v) + gkv*n^4*(vk - v) + gkc * c/(1+c) * (vk - v) + gl
*(vl-v) + I
dn/dt = (ninfty(v) - n)/taun(v)
dc/dt = rho*(m(v)^3*h(v)*(vc - v) - kc*c)


# PARAMETERS
param vi=100, vk=-75, vl=-40, vc=100
param gi=1800, gkv=1700, gkc=11.5, gl=7
param I = 0
```

```
param kc = 0.03
param rho = .27
param lambda = 400

# infinity
m(v) = alpham(v)/(alpham(v)+betam(v))
alpham(v) = 0.1*(25+v)/(1-exp(-.1*v-2.5))
betam(v) = 4*exp(-(v+50)/18)
h(v) = alphah(v)/(alphah(v)+betah(v))
alphah(v) = 0.07*exp(-0.05*v-2.5)
betah(v) = 1/(1+exp(-0.1*v-2))
ninfty(v) = alphan(v)/(alphan(v)+betan(v))
alphan(v) = 0.01*(20+v)/(1-exp(-.1*v-2))
betan(v) = 0.125*exp(-(v+30)/80)
taun(v) = 1/ (lambda*(alphan(v) + betan(v)))



@ TOTAL=40,DT=0.01,XLO=0,XHI=40,YLO=-60,YHI=0

done
```

Appendix D

XPP Code For Chay Model on Energy Consumption

```
# EQUATIONS

dv/dt = gi*m(v)^3*h(v)*(vi - v) + gkv*n^4*(vk - v) + gkc * c/(1+c) * (vk - v) + gl
*(vl-v) + I
dn/dt = (ninfty(v) - n)/taun(v)
dc/dt = rho*(m(v)^3*h(v)*(vc - v) - kc*c)
dp/dt = abs(ikv(v)*vk)+abs(ikc(v)*vk)+abs(il(v)-vl)-abs(ii(v)*vi)


# PARAMETERS
param vi=100, vk=-75, vl=-40, vc=100
```

```
param gi=1800, gkv=1700, gkc=11.5, gl=7
param I = 0
param kc = 0.03
param rho = .27
param lambda = 400

# infinity
m(v) = alpham(v)/(alpham(v)+betam(v))
alpham(v) = 0.1*(25+v)/(1-exp(-.1*v-2.5))
betam(v) = 4*exp(-(v+50)/18)
h(v) = alphah(v)/(alphah(v)+betah(v))
alphah(v) = 0.07*exp(-0.05*v-2.5)
betah(v) = 1/(1+exp(-0.1*v-2))
ninfty(v) = alphan(v)/(alphan(v)+betan(v))
alphan(v) = 0.01*(20+v)/(1-exp(-.1*v-2))
betan(v) = 0.125*exp(-(v+30)/80)
taun(v) = 1/ (lambda*(alphan(v) + betan(v)))
#current
ii(v) = gi*m(v)^3*h(v)*(v-vi)
ikv(v) = gkv*n^4*(v-vk)
ikc(v) = gkc*(c/(1+c))*(v-vk)
il(v) = gl*(v-vi)
@ TOTAL=40,DT=0.01,XLO=0,XHI=40,YLO=-60,YHI=0
done
```